Report Figures and Tables Appendix

List of Tables

1 Constrained parameters of Ball-and-Stick model at voxel (92, 65). . . . 3
2 Best fitted parameters and their deviation after Ball-and-Stick stochastic starting point fitting in voxel (92, 65). . 3
3 Resnorm and parameters with different transformations. . . . 3
4 Computational time comparison with positive transformations and informed starting point. . . . 9
5 Classic bootstrap parameter distribution and its ranges. . . . 18
6 MCMC MH parameter distribution and its ranges. . . . 18
7 Ball-and-Stick best parameters for ISBI 2015 dataset. . . . 24
8 Diffusion tensor best parameters for ISBI 2015 dataset. . . . 24
9 Zeppelin-and-Stick best parameters for ISBI 2015 dataset. . . . 30
10 Zeppelin-and-Stick-with-Tortuosity best parameters for ISBI 2015 dataset. . . . 30
11 Resnorm comparison across four models for ISBI 2015 dataset. . . . 30
12 Information criteria of four models for ISBI 2015 dataset. . . . 30
13 Ball-and-Two-Stick best parameters for ISBI 2015 dataset. . . . 30
14 Information criteria of five models for ISBI 2015 dataset. . . . 30
15 AIC and BIC comparison of best models for each voxel in ISBI 2015 dataset. . . . 31
16 Cross-validation results of best models for each fold in ISBI 2015 dataset. . . . 31

List of Figures

1 Mean diffusivity at slice 72 after weighted linear diffusion tensor fitting. . . . 4
2 Fractional anisotropy at slice 72 after weighted linear diffusion tensor fitting. . . . 5
3 Directionally-encoded color map at slice 72 after weighted linear diffusion tensor fitting. Red represents left-right, green represents anterior-posterior, and blue represents superior-inferior. . . . 6
4 Unconstrained Ball-and-Stick model measurement (black square) vs prediction (red cross). . . . 7
5 Constrained Ball-and-Stick model Measurement (black square) vs prediction (red cross). . . . 7
6 Distribution of starting point parameters after applying normal noise. . . . 8
7 Resnorm distribution after Ball-and-Stick stochastic starting point fitting in voxel (92, 65). . . . 8
8 Parameter distribution after Ball-and-Stick stochastic starting point fitting in voxel (92, 65). . . . 9
9 Location of other voxels dispersed around the brain slice. Colours are used for after when referencing other voxels. Red (92, 65), green (100, 125), blue (40, 45), cyan (60, 130), magenta (72, 52), yellow (61, 95). . . . 10
10 Sample figure caption. . . . 11
11 Resnorm mapping slice 72 with Ball-and-Stick model and constrained settings. . . . 12
12 S_0 mapping of slice 72 with Ball-and-Stick model and constrained settings. . . . 13
13 Diffusivity d mapping of slice 72 with Ball-and-Stick model and constrained settings. . . . 14
14 Fraction f mapping of slice 72 with Ball-and-Stick model and constrained settings. . . . 15
15 Weighted fibre direction mapping of slice 72 with Ball-and-Stick model and constrained settings. . . . 16
16 Zoomed weighted fibre direction mapping of slice 72 with Ball-and-Stick model and constrained settings. . . . 17
17 Classic bootstrap resnorm and parameter distribution of voxel (92, 65). Dotted lines - $2-\sigma$ range, dashed lines - 95% range. Same convention used for following figures. . . . 18
18 Classic bootstrap resnorm and parameter distribution of voxel (100, 125). . . . 19
19 Classic bootstrap resnorm and parameter distribution of voxel (40, 45). . . . 19

20 Classic bootstrap resnorm and parameter distribution of voxel (61, 95). 20
21 Acceptance rate every 100 of MCMC samples with initial perturbation settings, voxel (92, 65). 20
22 Acceptance rate every 100 of MCMC samples with refined perturbation settings, voxel (92, 65). 21
23 MCMC MH resnorm and parameter distribution of voxel (92, 65). 21
24 Acceptance rate every 100 of MCMC samples with initial perturbation settings, voxel (100, 125). 22
25 MCMC MH resnorm and parameter distribution of voxel (100, 125). 22
26 Laplace approximation resnorm and parameter distribution of voxel (92, 65). 23
27 Parametric bootstrap resnorm and parameter distribution of voxel (92, 65). 23
28 Ball-and-Stick resnorm distribution for ISBI 2015 dataset. 24
29 Ball-and-Stick model measurement (square) vs prediction (cross) for ISBI 2015 dataset. 25
30 Diffusion tensor model measurement (square) vs prediction (cross) for ISBI 2015 dataset. 25
31 Zeppelin-and-Stick model first attempt resnorm distribution for ISBI 2015 dataset. 26
32 Zeppelin-and-Stick model refined resnorm distribution for ISBI 2015 dataset. 26
33 Zeppelin-and-Stick model refined measurement (square) vs prediction (cross) for ISBI 2015 dataset. 27
34 Zeppelin-and-Stick-with-Tortuosity model resnorm distribution for ISBI 2015 dataset. 27
35 Zeppelin-and-Stick-with-Tortuosity model measurement (square) vs prediction (cross) for ISBI 2015 dataset. . 28
36 Ball-and-Two-Stick resnorm distribution for ISBI 2015 dataset. 28
37 Ball-and-Two-Stick model measurement (square) vs prediction (cross) for ISBI 2015 dataset. 29
38 AICc mapping for the best model in HARDI slice 72 29
39 Akaike weighted AICc mapping for the best model in HARDI slice 72 31

1 Figure and Tables

Table 1: Constrained parameters of Ball-and-Stick model at voxel (92, 65).

Parameter	**Value**
ResNorm	5.8720e+06
S_0	4.2579e+03
d	1.1413e-03
f	3.5731e-01
θ	-9.8107e-01
ϕ	5.7945e-01

Table 2: Best fitted parameters and their deviation after Ball-and-Stick stochastic starting point fitting in voxel (92, 65).

Parameter	**Value**	**Standard Deviation**
S_0	4.2579e+03	5.3808e-05
d	1.1413e-03	2.2881e-11
f	3.5731e-01	1.6713e-08
θ	9.8107e-01	3.8644e-01
ϕ	-2.5621e+00	6.1873e-01

Table 3: Resnorm and parameters with different transformations.

Positive	**Angles**	**S(0)**	**d**	**f**	θ	ϕ	**RESNORM**
Exponential	True	4.2583e+03	7.7055e-04	1.8642e-10	0	0	1.5690e+07
Squared	True	4.2583e+03	7.7055e-04	8.6088e-13	0	0	1.5690e+07
Exponential	False	4.2579e+03	1.1413e-03	3.5731e-01	-9.8107e-01	5.7945e-01	5.8720e+06
Squared	False	4.2579e+03	1.1413e-03	3.5731e-01	-9.8107e-01	5.7945e-01	5.8720e+06

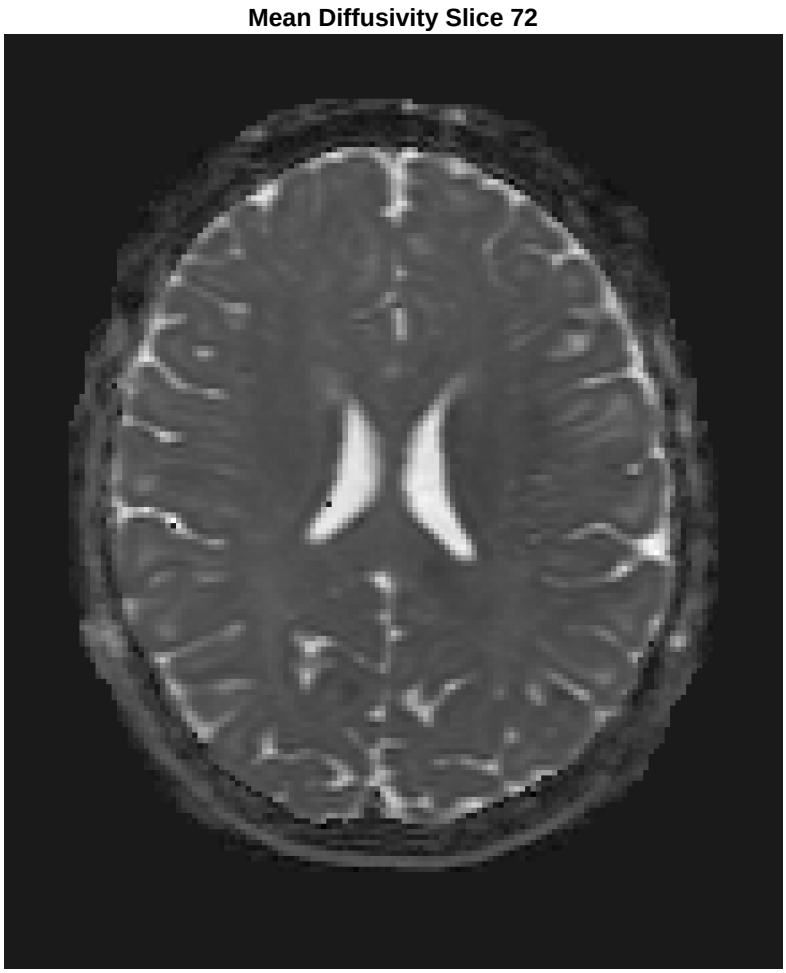

Figure 1: Mean diffusivity at slice 72 after weighted linear diffusion tensor fitting.

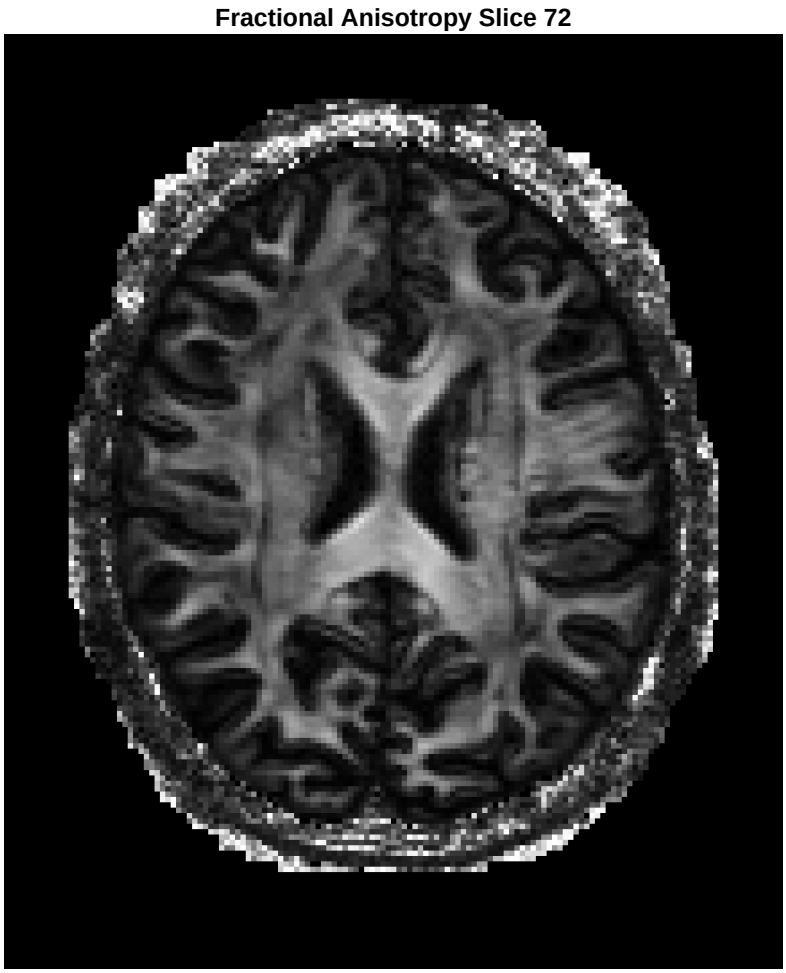

Figure 2: Fractional anisotropy at slice 72 after weighted linear diffusion tensor fitting.

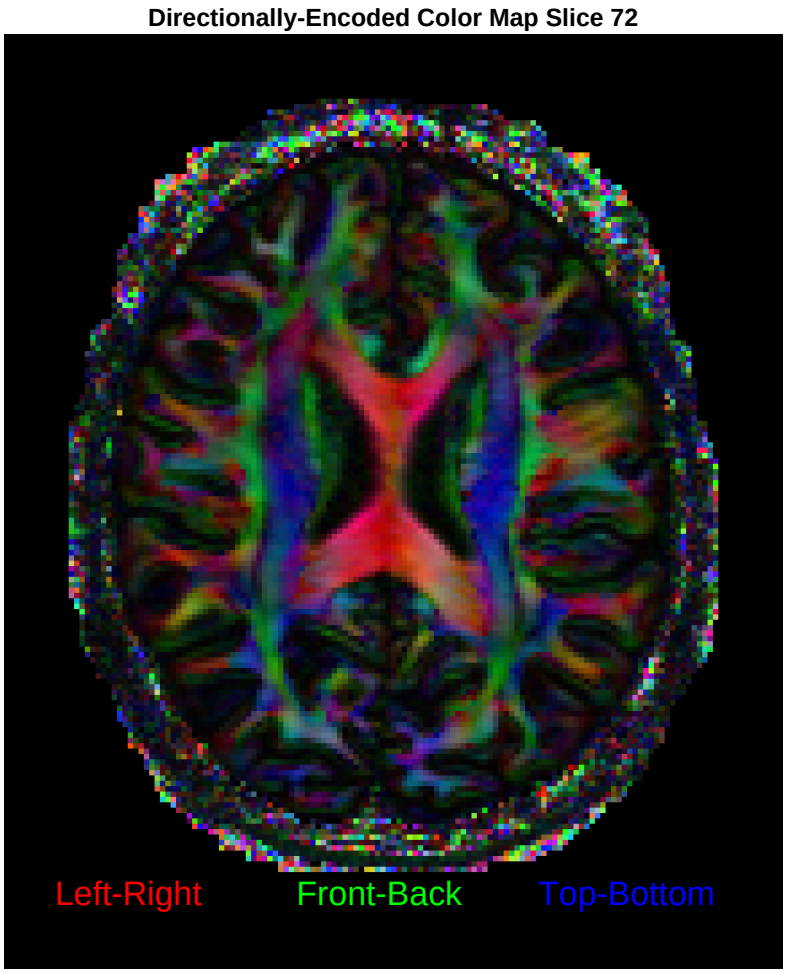

Figure 3: Directionally-encoded color map at slice 72 after weighted linear diffusion tensor fitting. Red represents left-right, green represents anterior-posterior, and blue represents superior-inferior.

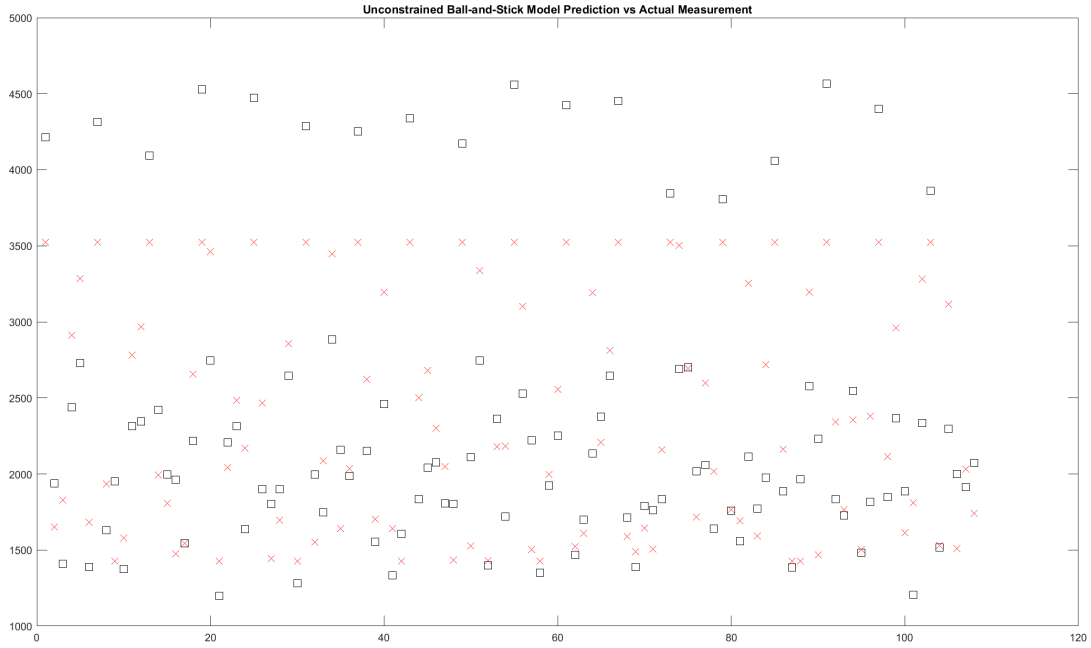

Figure 4: Unconstrained Ball-and-Stick model measurement (black square) vs prediction (red cross).

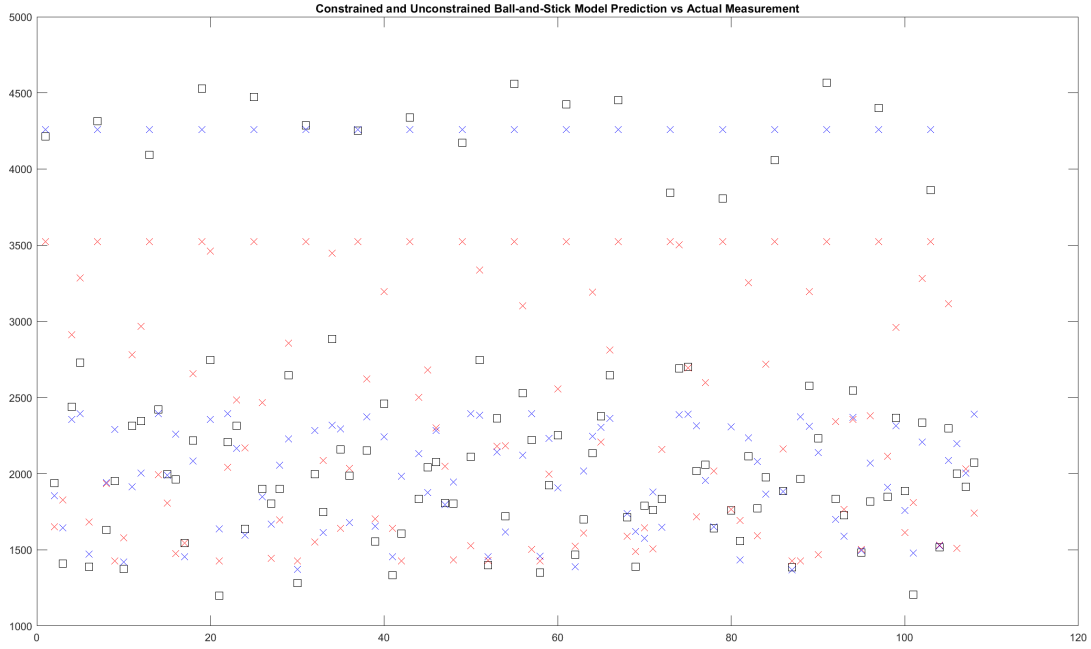

Figure 5: Constrained Ball-and-Stick model Measurement (black square) vs prediction (red cross).

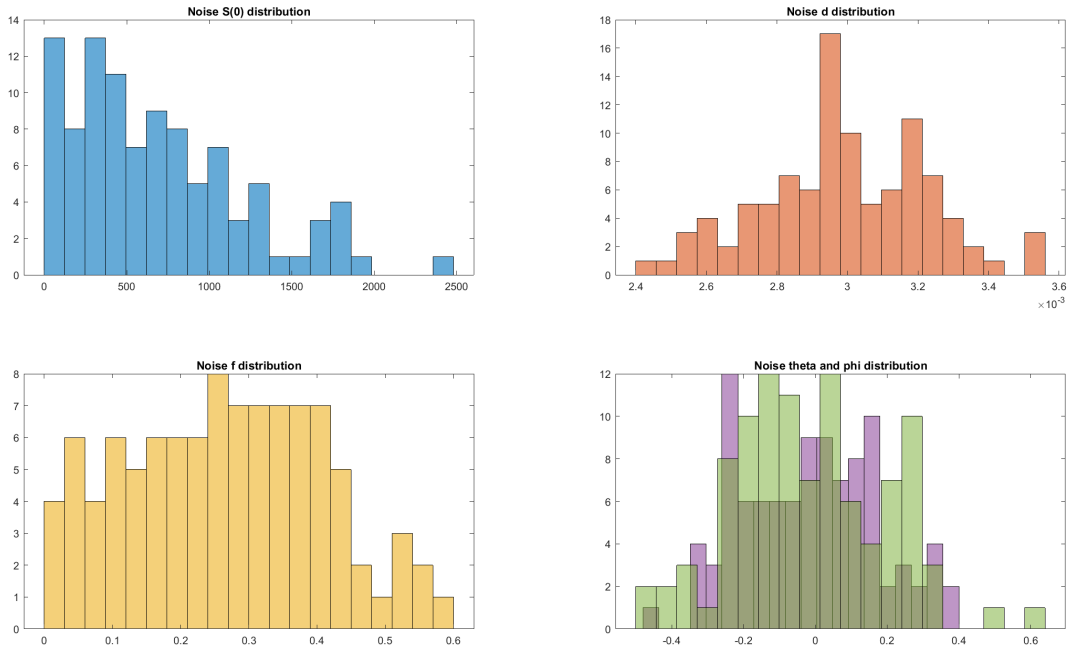

Figure 6: Distribution of starting point parameters after applying normal noise.

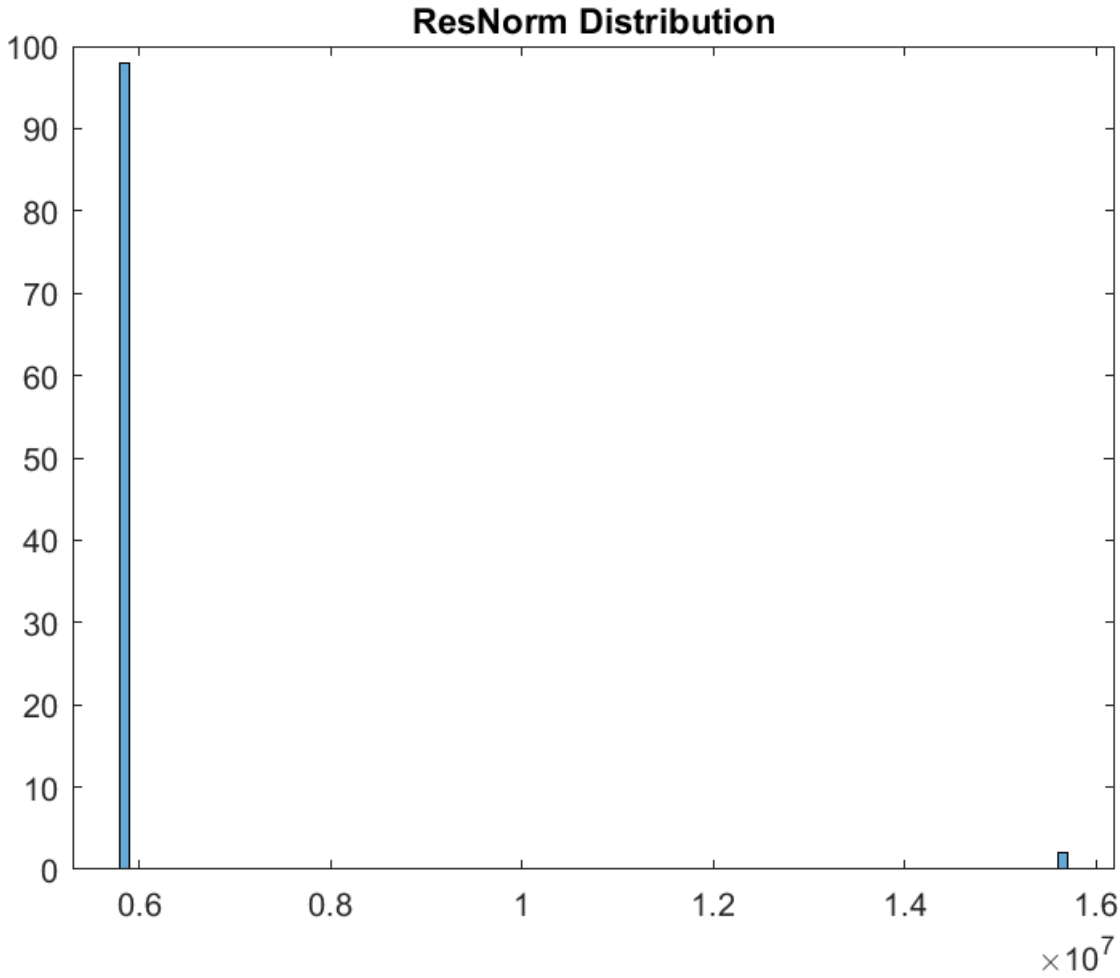

Figure 7: Resnorm distribution after Ball-and-Stick stochastic starting point fitting in voxel (92, 65).

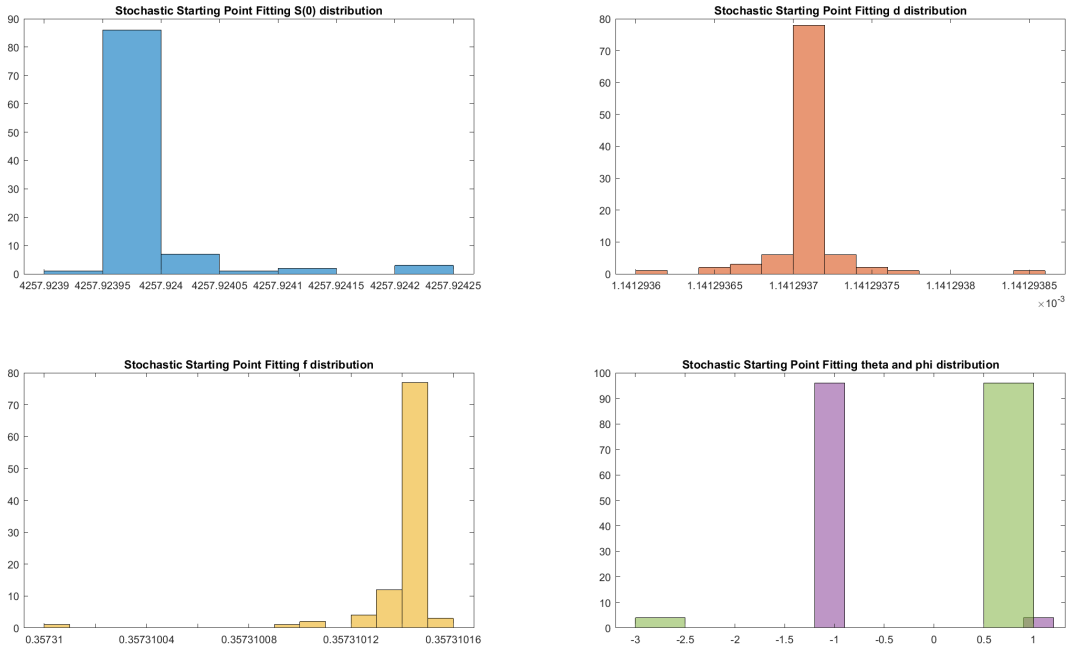

Figure 8: Parameter distribution after Ball-and-Stick stochastic starting point fitting in voxel (92, 65).

Table 4: Computational time comparison with positive transformations and informed starting point.

Positive Transform	**Informed Starting Point**	**Time in s**
Exponential	No	397.42
Exponential	Yes	593.36
Squared	No	1432.36
Squared	Yes	1174.68

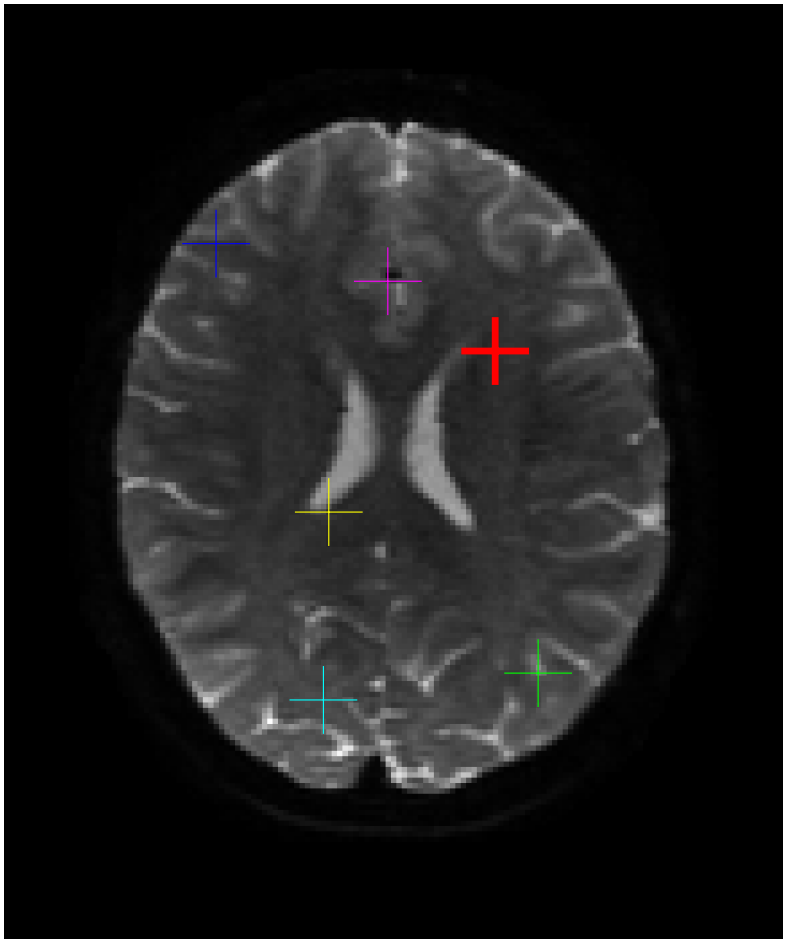

Figure 9: Location of other voxels dispersed around the brain slice. Colours are used for after when referencing other voxels. Red (92, 65), green (100, 125), blue (40, 45), cyan (60, 130), magenta (72, 52), yellow (61, 95).

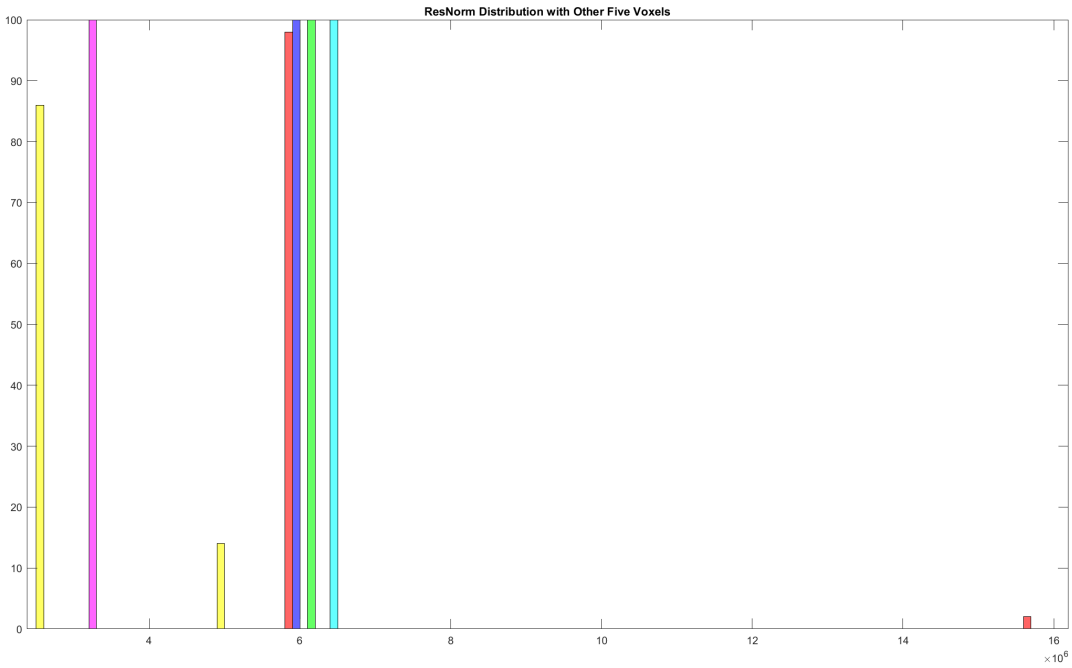

Figure 10: Sample figure caption.

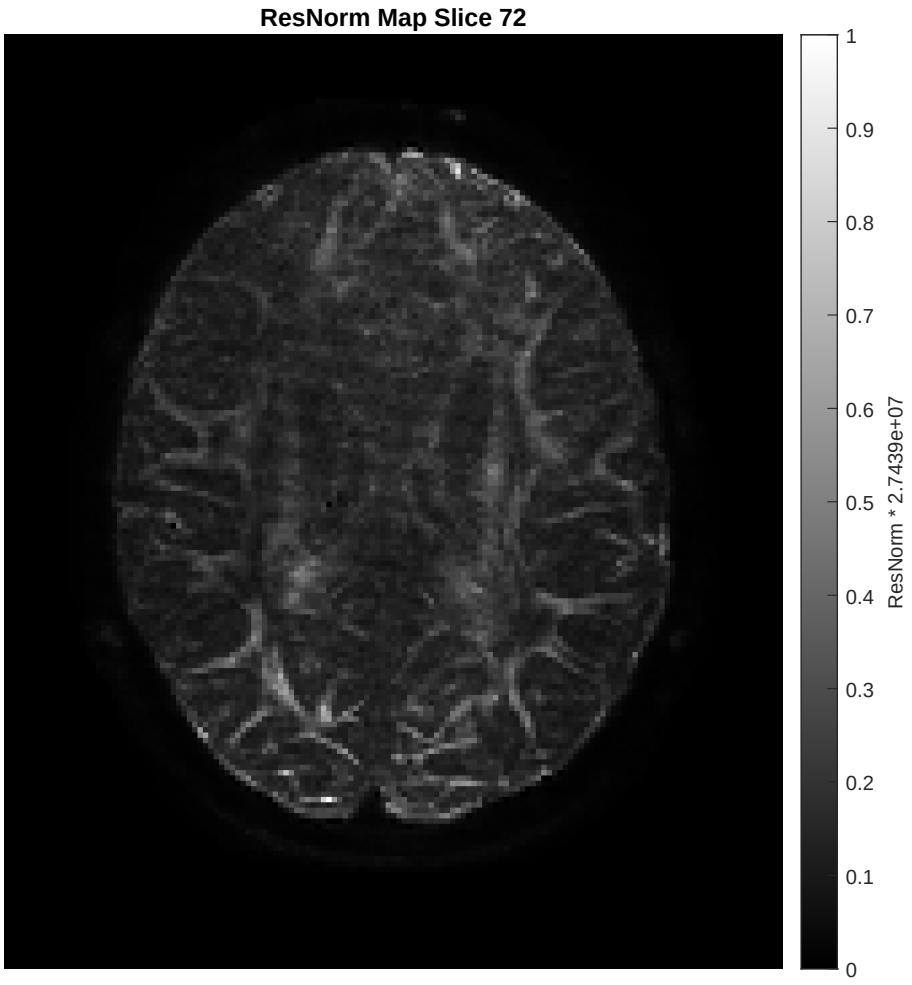

Figure 11: Resnorm mapping slice 72 with Ball-and-Stick model and constrained settings.

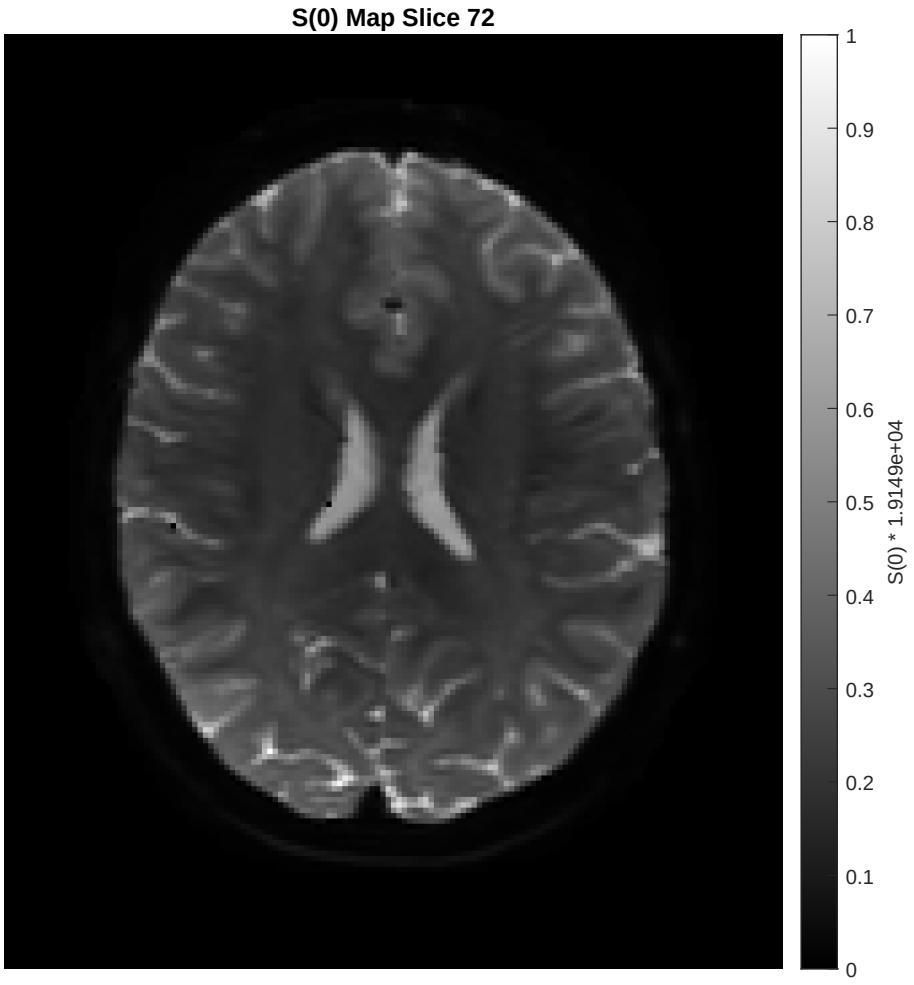

Figure 12: S_0 mapping of slice 72 with Ball-and-Stick model and constrained settings.

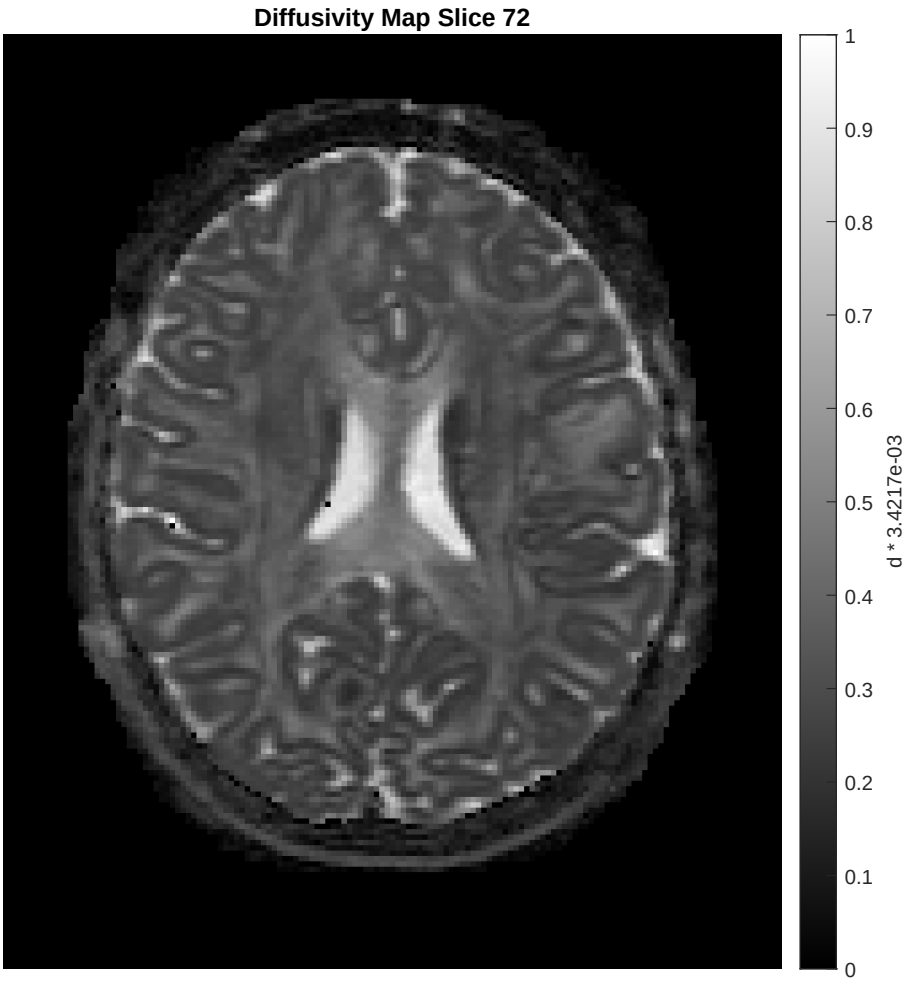

Figure 13: Diffusivity d mapping of slice 72 with Ball-and-Stick model and constrained settings.

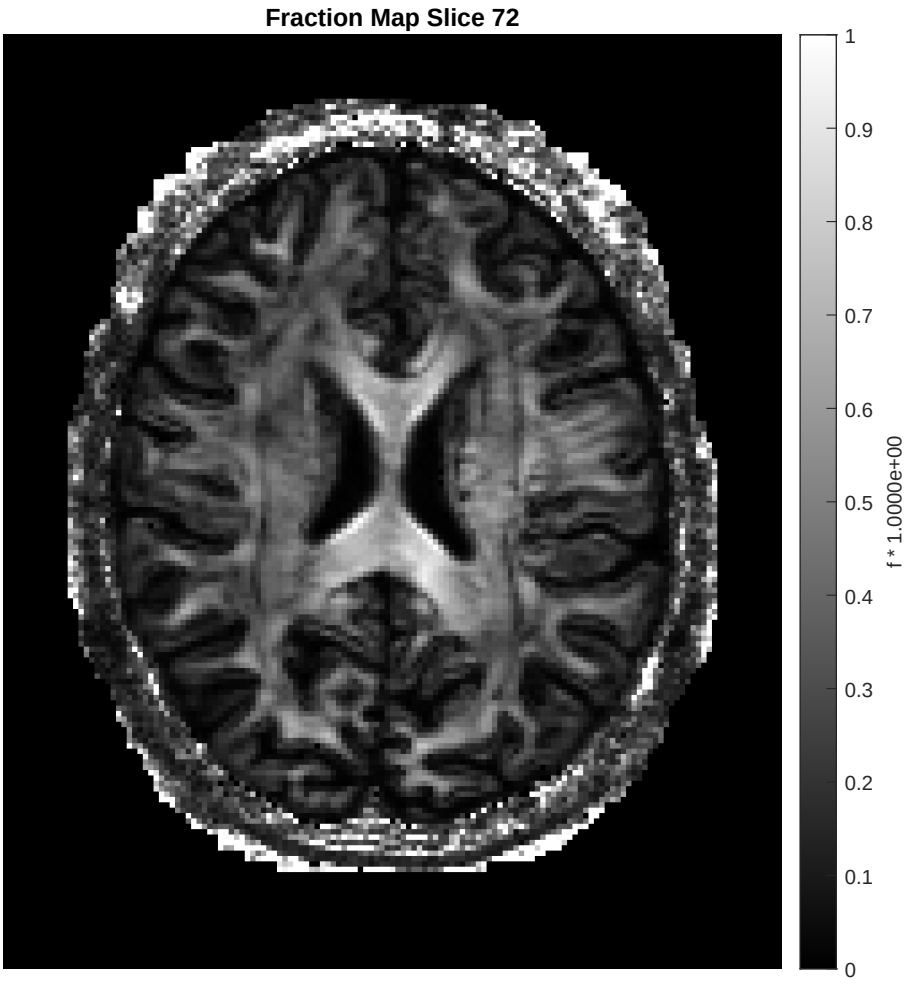

Figure 14: Fraction f mapping of slice 72 with Ball-and-Stick model and constrained settings.

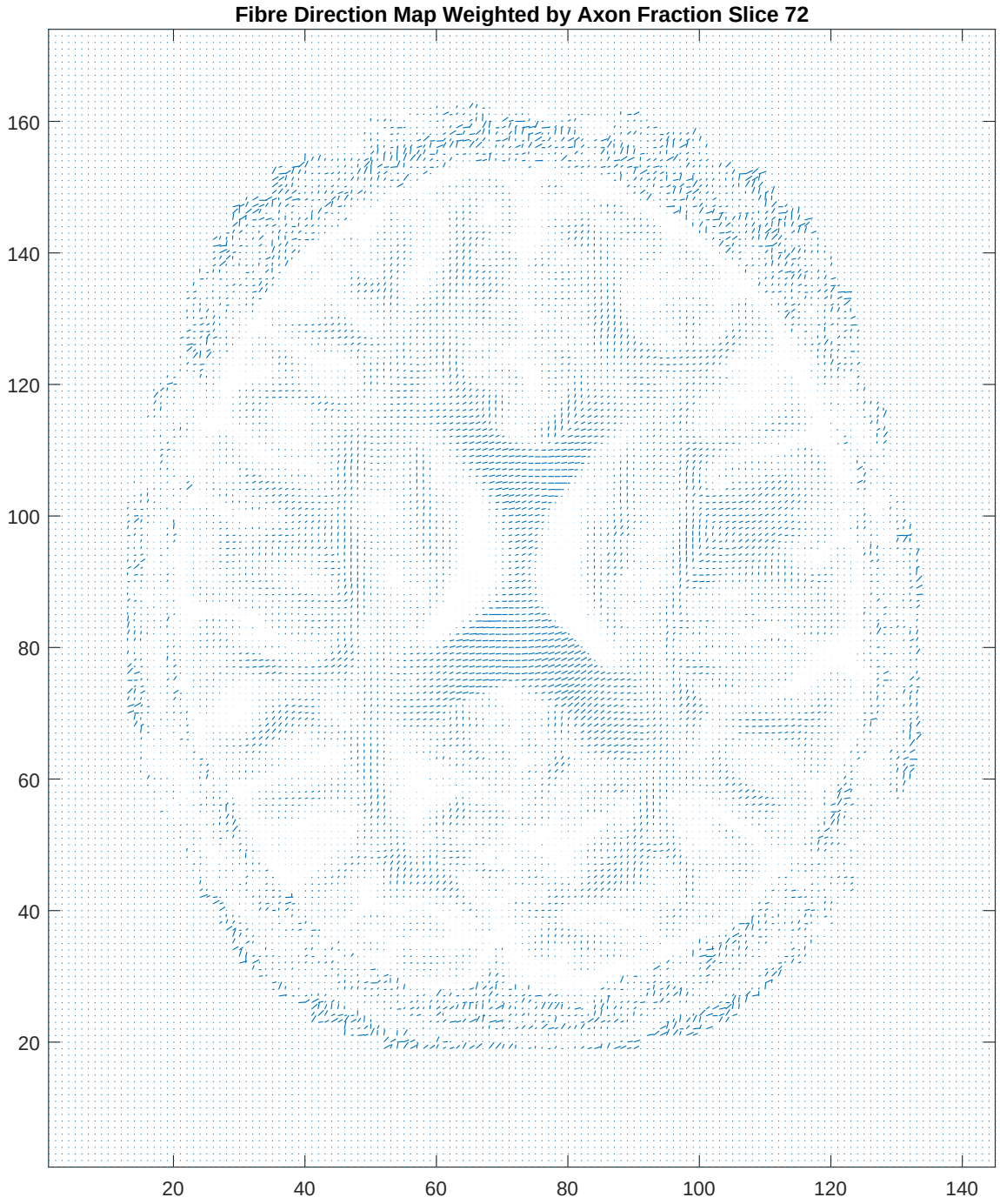

Figure 15: Weighted fibre direction mapping of slice 72 with Ball-and-Stick model and constrained settings.

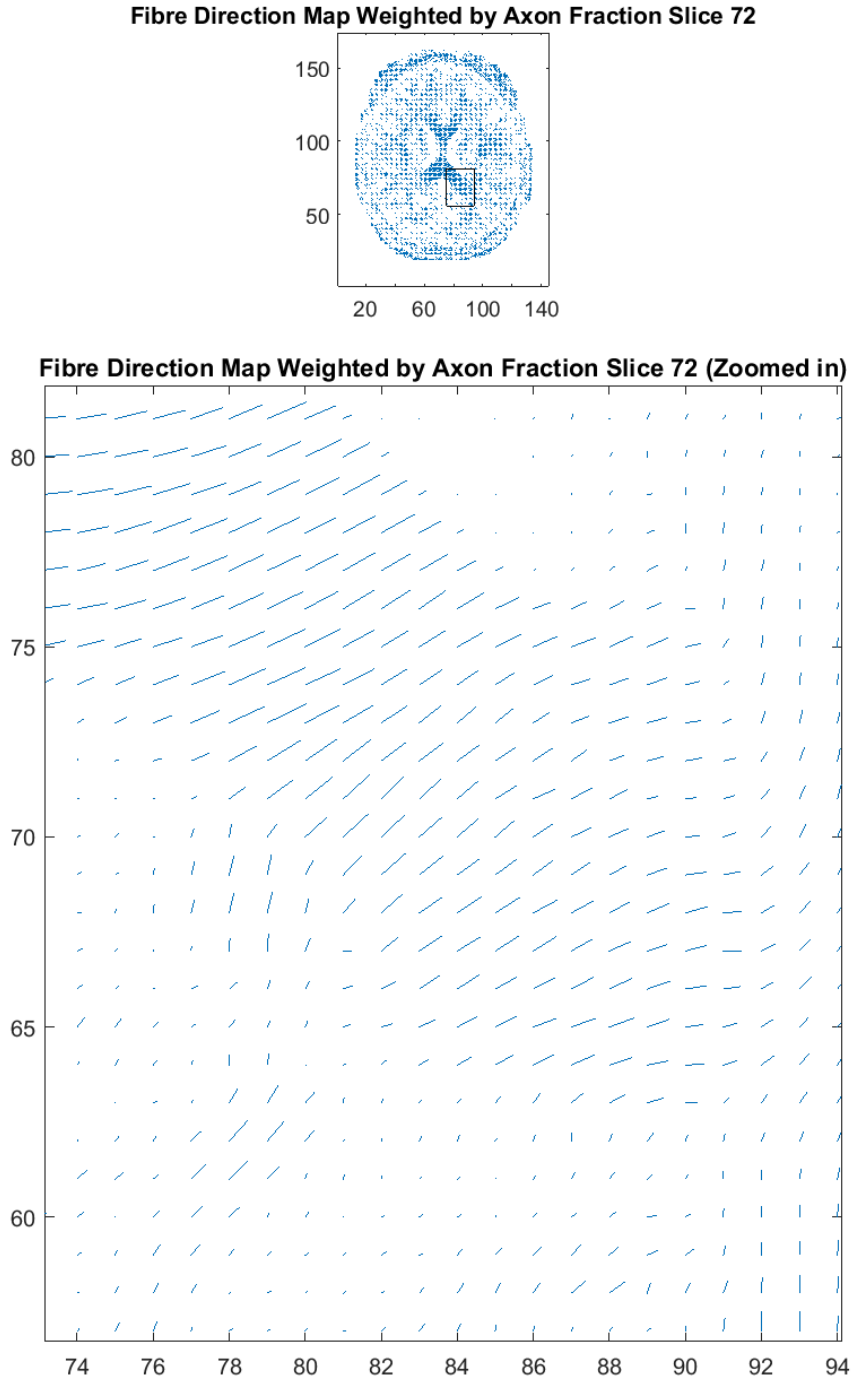

Figure 16: Zoomed weighted fibre direction mapping of slice 72 with Ball-and-Stick model and constrained settings.

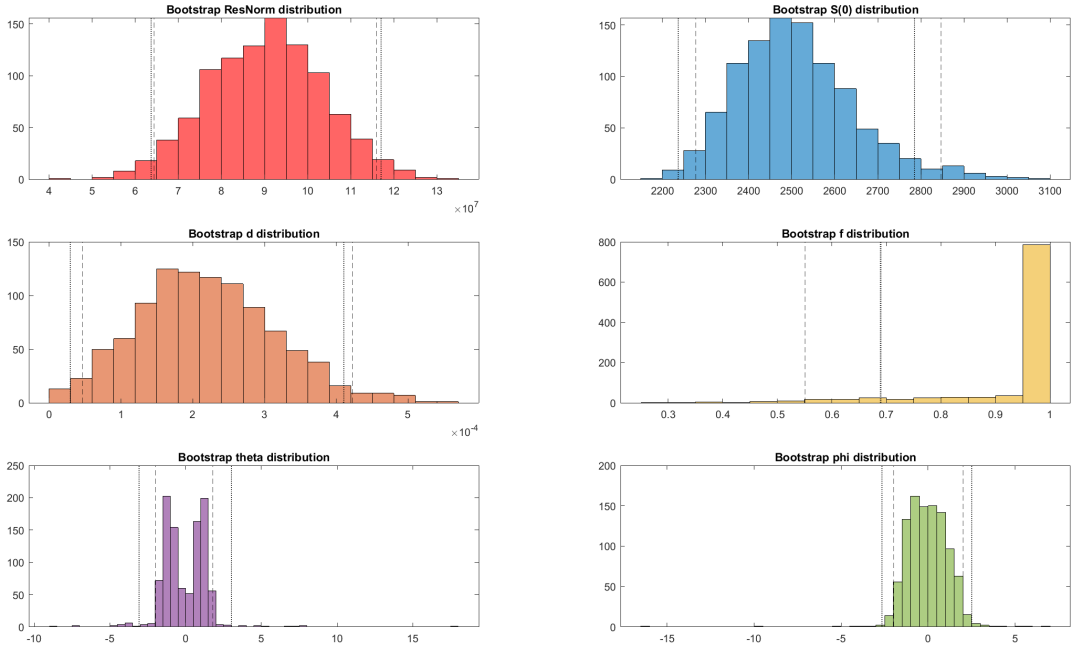

Figure 17: Classic bootstrap resnorm and parameter distribution of voxel (92, 65). Dotted lines - 2 − σ range, dashed lines - 95% range. Same convention used for following figures.

Table 5: Classic bootstrap parameter distribution and its ranges.

Parameter	**Left 2-σ**	**Right 2-σ**	**Left 95%**	**Right 95%**
ResNorm	6.3604e+07	1.1700e+08	6.4342e+07	1.1609e+08
S_0	2.2357e+03	2.7862e+03	2.2770e+03	2.8471e+03
d	2.8687e-05	4.1041e-04	4.6459e-05	4.2221e-04
f	6.8968e-01	1.1981e+00	5.5124e-01	1.0000e+00
θ	-3.0773e+00	2.9937e+00	-1.9779e+00	1.8008e+00
ϕ	-2.6280e+00	2.5266e+00	-1.9712e+00	2.0183e+00

Table 6: MCMC MH parameter distribution and its ranges.

Parameter	**Left 2-σ**	**Right 2-σ**	**Left 95%**	**Right 95%**
ResNorm	5.2090e+06	8.2482e+06	5.9916e+06	8.7489e+06
S_0	4.0876e+03	4.4356e+03	4.1008e+03	4.4346e+03
d	9.9732e-04	1.2612e-03	1.0049e-03	1.2594e-03
f	2.9546e-01	3.9437e-01	2.9713e-01	3.9241e-01
θ	8.9934e-01	1.0722e+00	9.0813e-01	1.0712e+00
ϕ	-2.7010e+00	-2.4417e+00	-2.6799e+00	-2.4347e+00

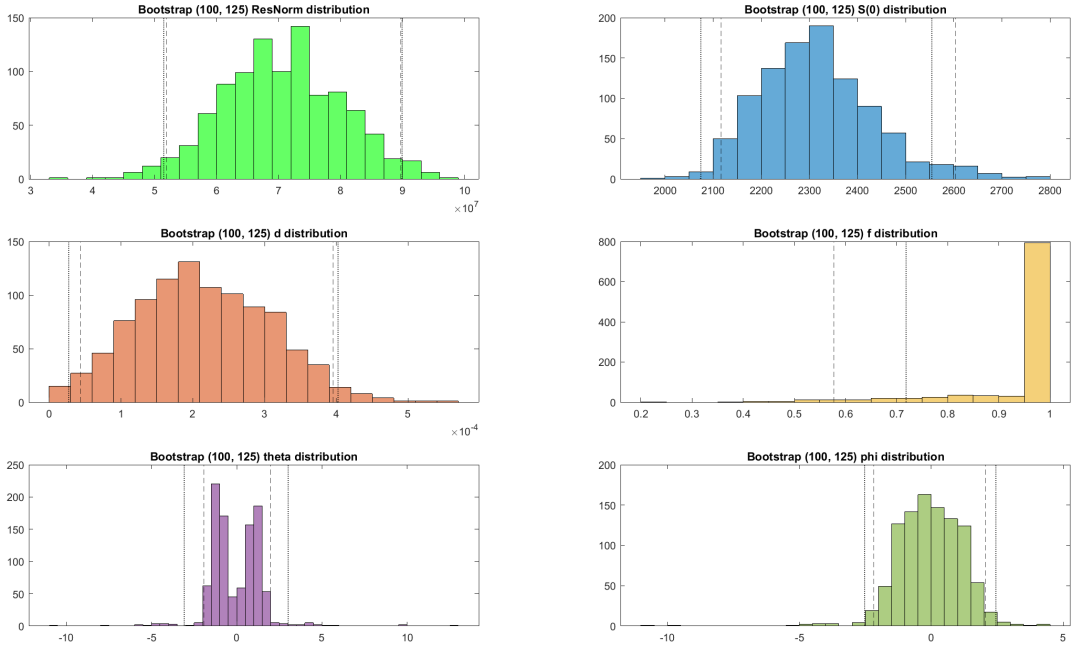

Figure 18: Classic bootstrap resnorm and parameter distribution of voxel (100, 125).

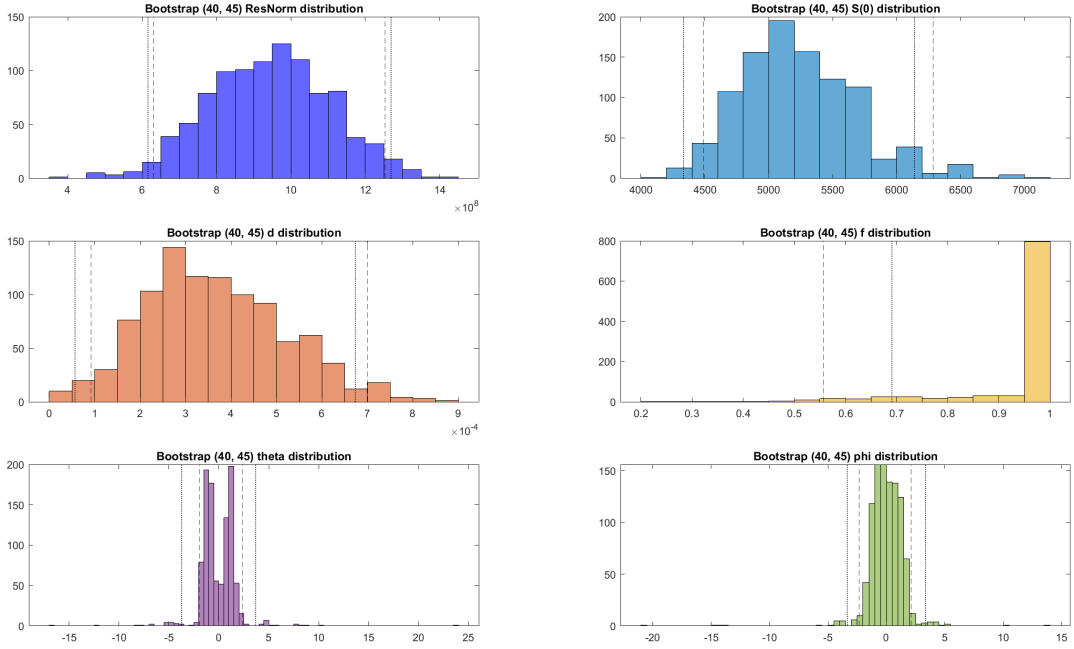

Figure 19: Classic bootstrap resnorm and parameter distribution of voxel (40, 45).

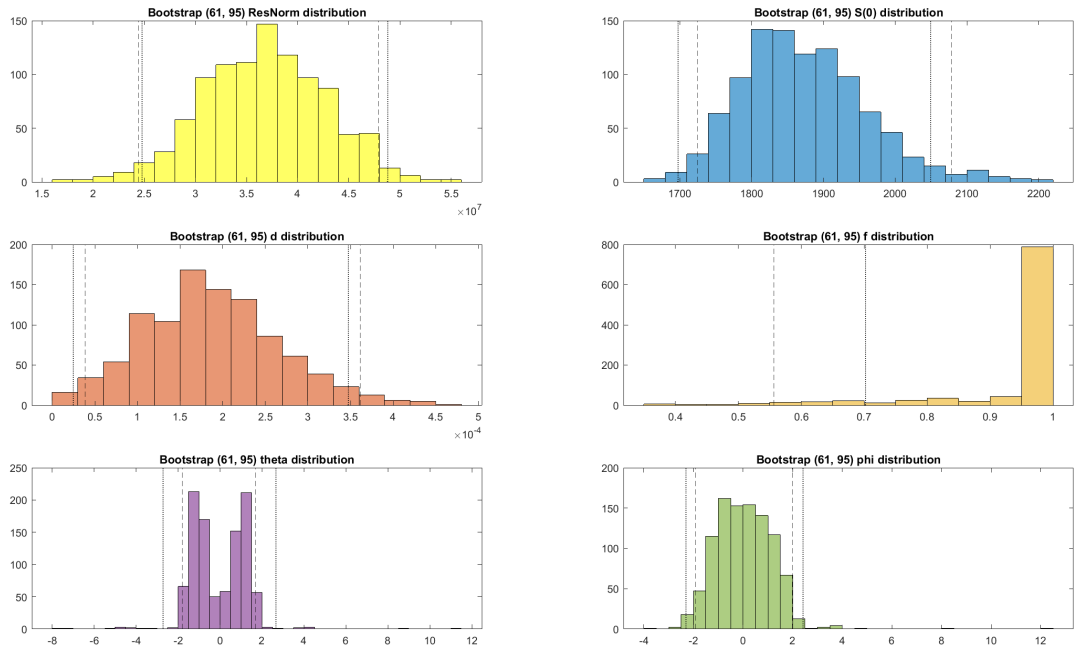

Figure 20: Classic bootstrap resnorm and parameter distribution of voxel (61, 95).

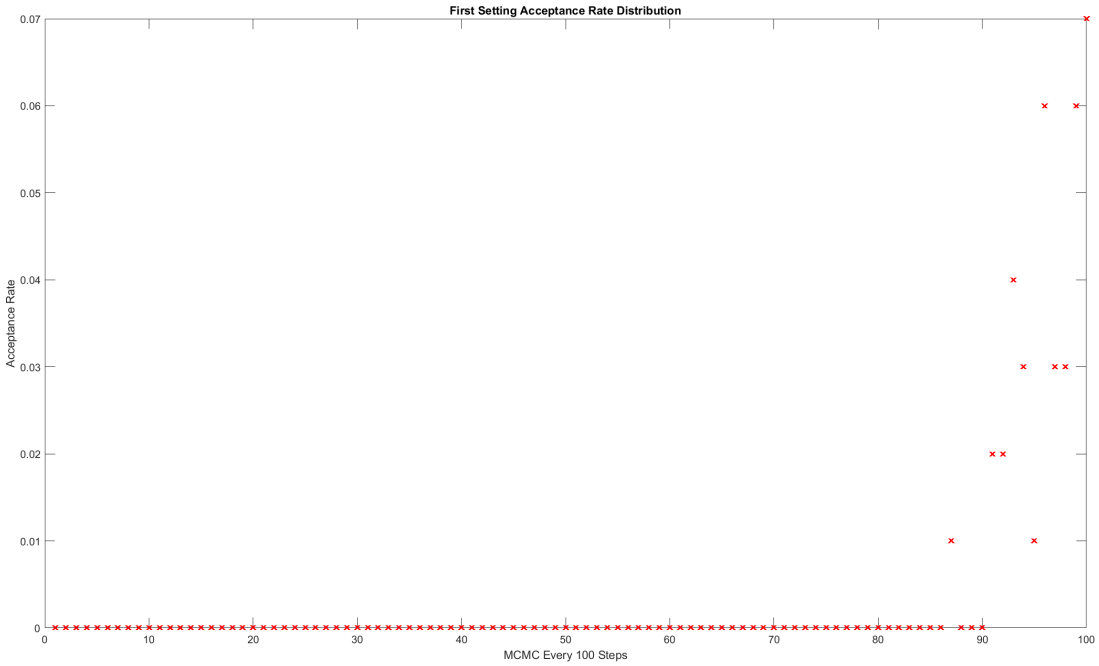

Figure 21: Acceptance rate every 100 of MCMC samples with initial perturbation settings, voxel (92, 65).

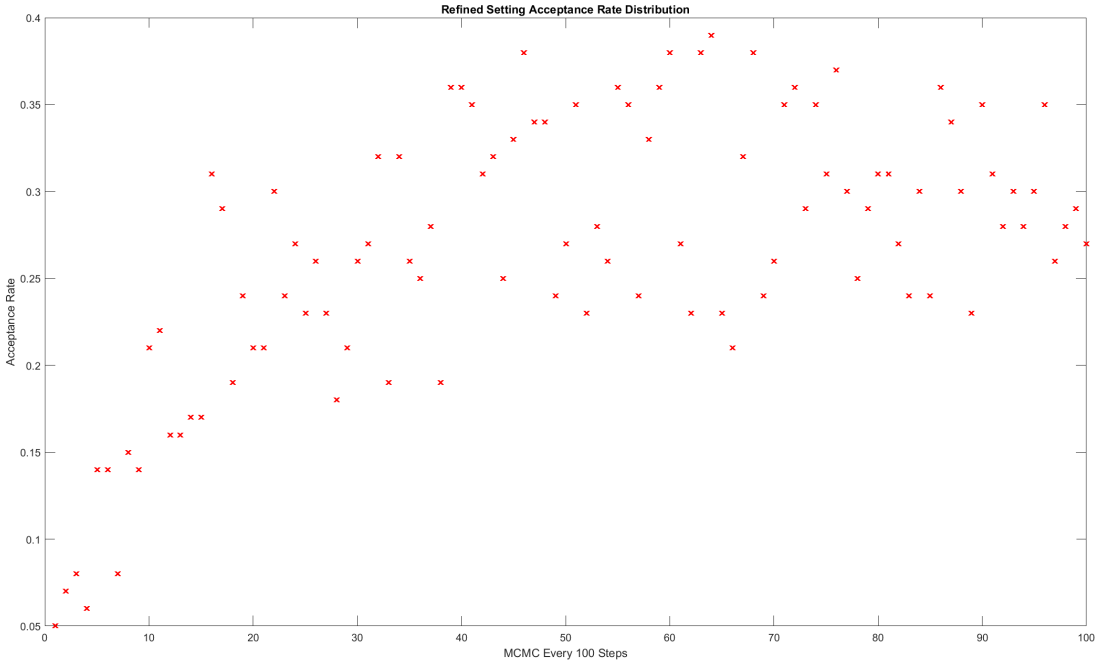

Figure 22: Acceptance rate every 100 of MCMC samples with refined perturbation settings, voxel (92, 65).

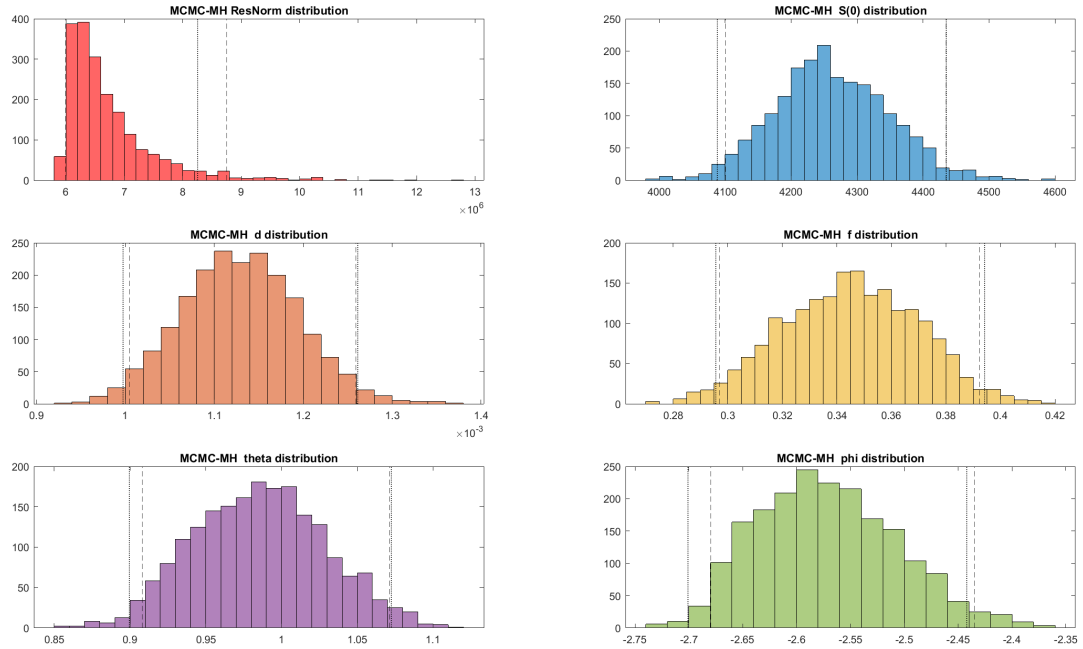

Figure 23: MCMC MH resnorm and parameter distribution of voxel (92, 65).

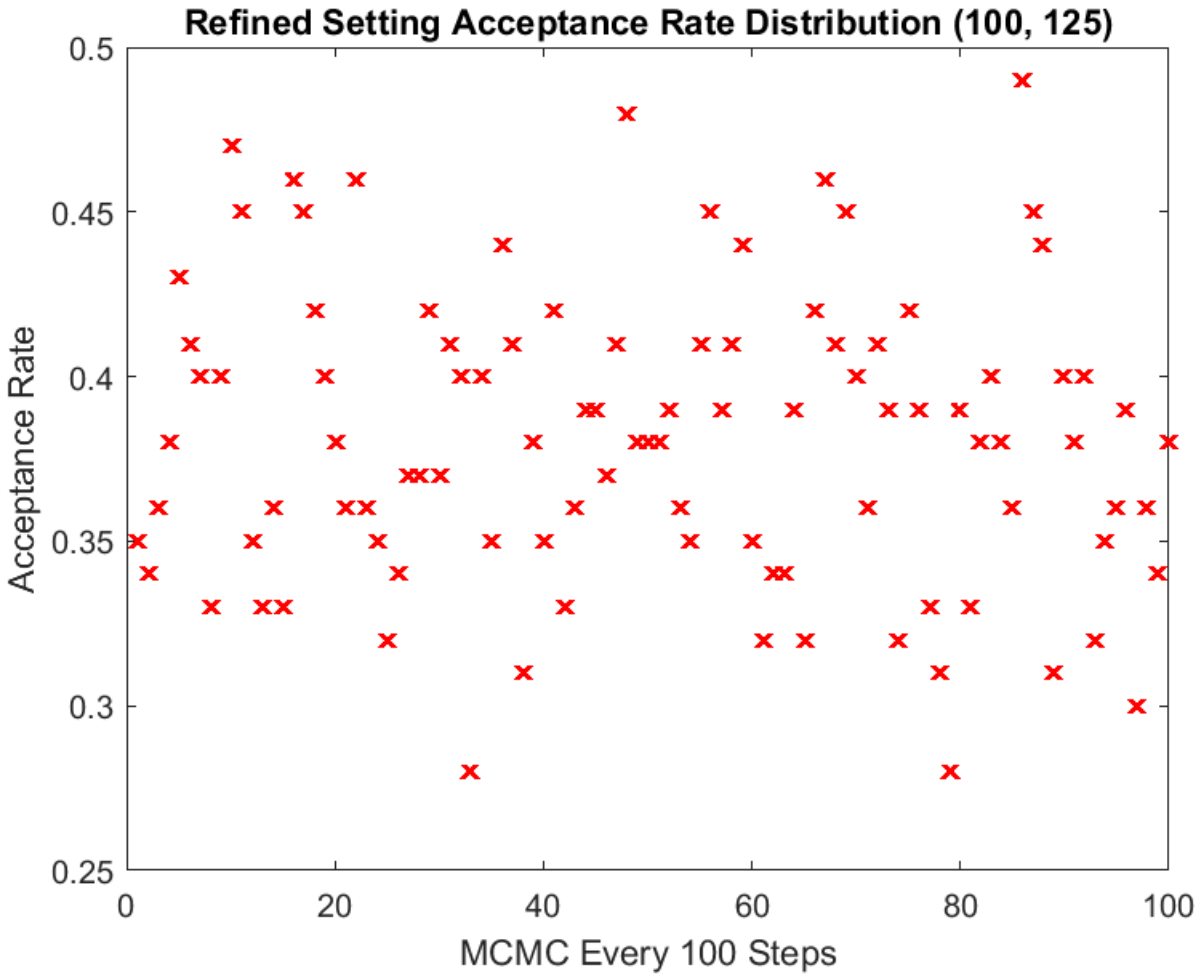

Figure 24: Acceptance rate every 100 of MCMC samples with initial perturbation settings, voxel (100, 125).

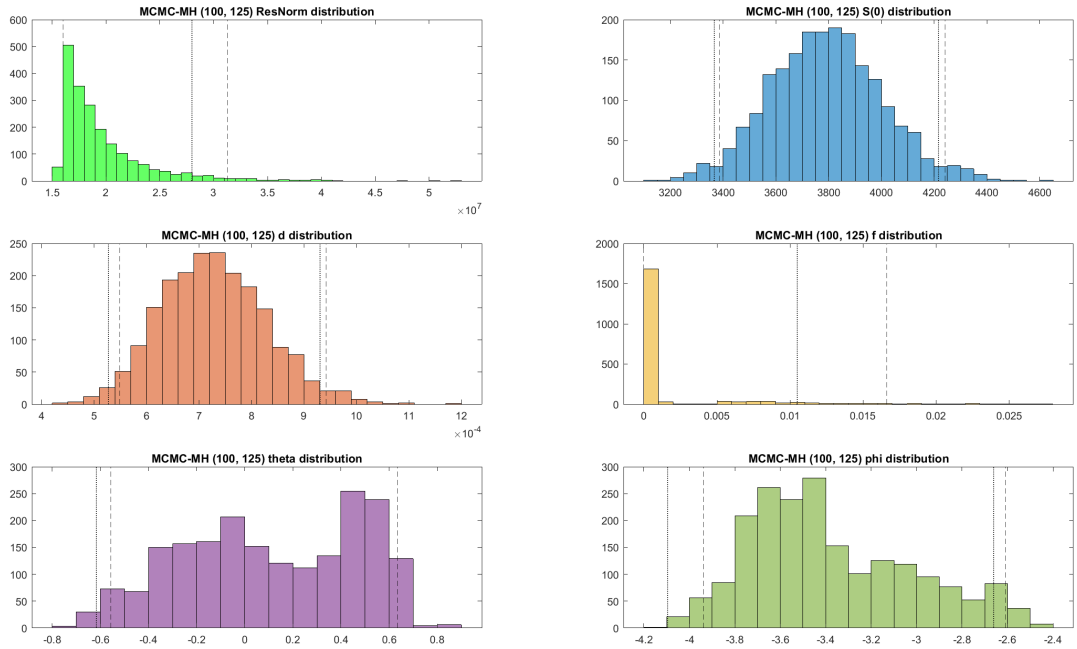

Figure 25: MCMC MH resnorm and parameter distribution of voxel (100, 125).

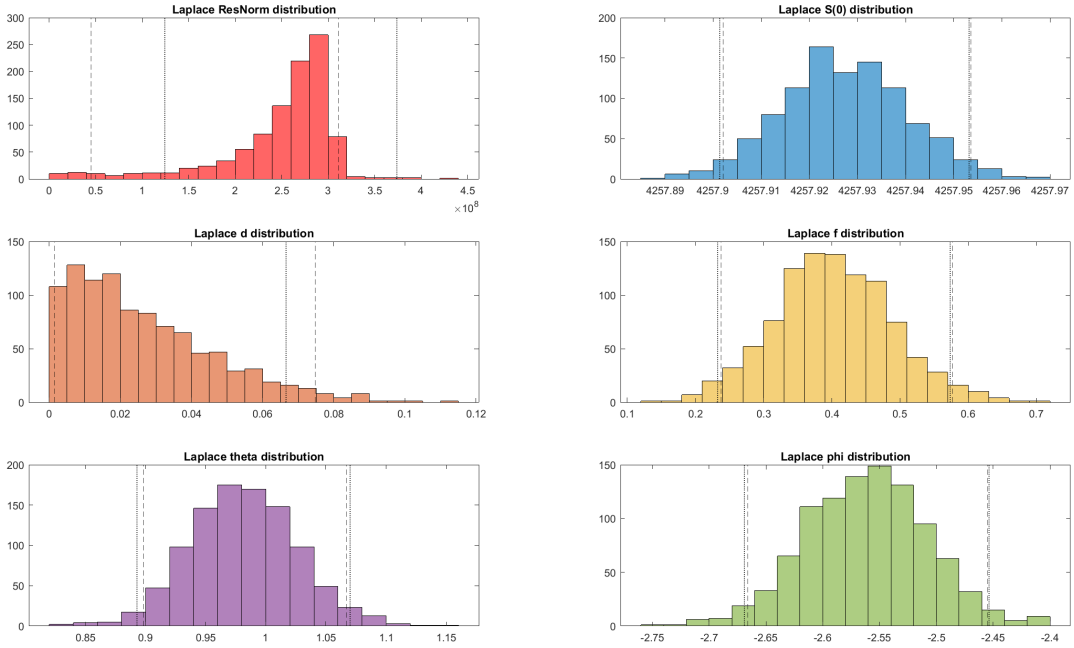

Figure 26: Laplace approximation resnorm and parameter distribution of voxel (92, 65).

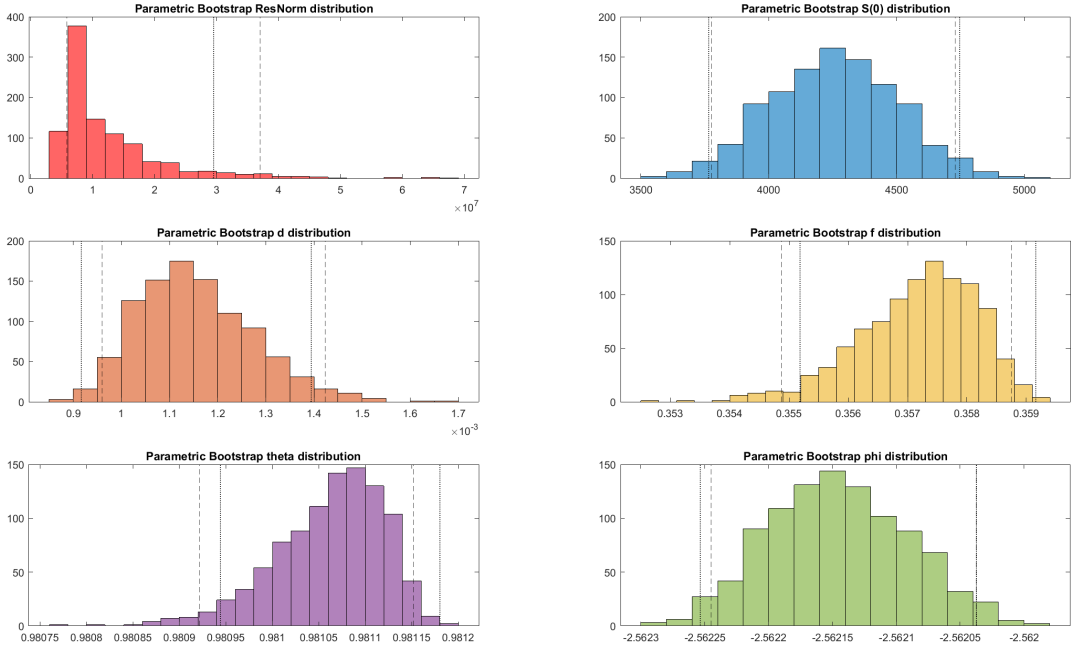

Figure 27: Parametric bootstrap resnorm and parameter distribution of voxel (92, 65).

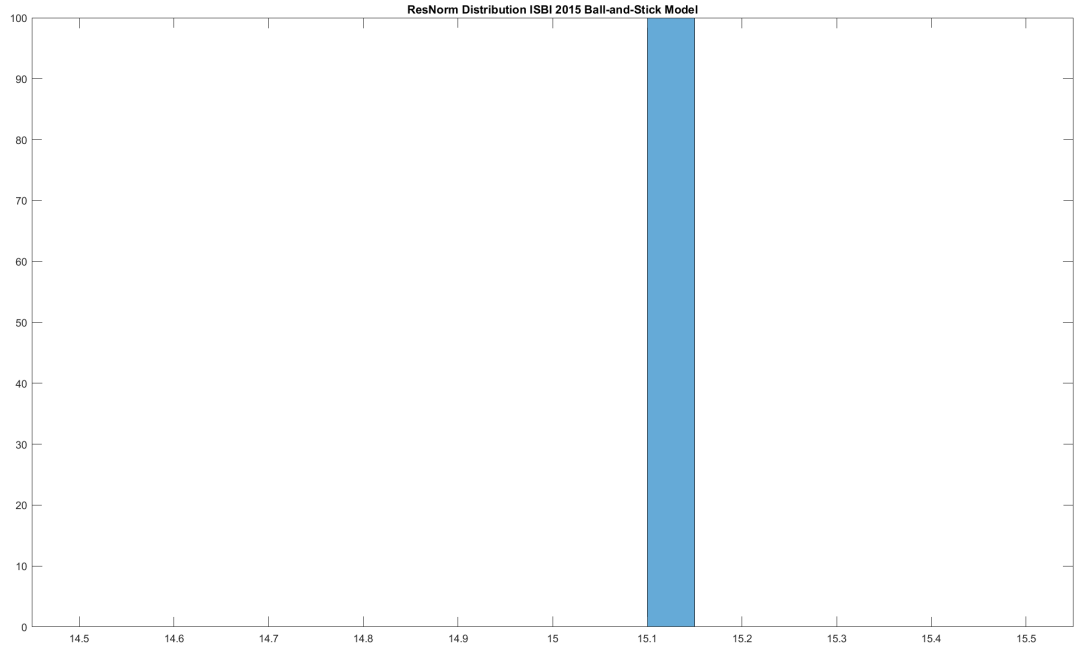

Figure 28: Ball-and-Stick resnorm distribution for ISBI 2015 dataset.

Table 7: Ball-and-Stick best parameters for ISBI 2015 dataset.

Parameter	**Value**
ResNorm	1.5106e+01
S_0	1.0099e+00
d	1.4321e-03
f	5.7493e-01
θ	-1.5447e+00
ϕ	-8.2863e-02

Table 8: Diffusion tensor best parameters for ISBI 2015 dataset.

Parameter	**Value**
ResNorm	1.8191e+01
S_0	9.6381e-01
D_{xx}	1.6649e-03
D_{xy}	-1.5677e-04
D_{xz}	-3.1417e-05
D_{yy}	1.5374e-04
D_{yz}	2.0719e-05
D_{zz}	1.6040e-04

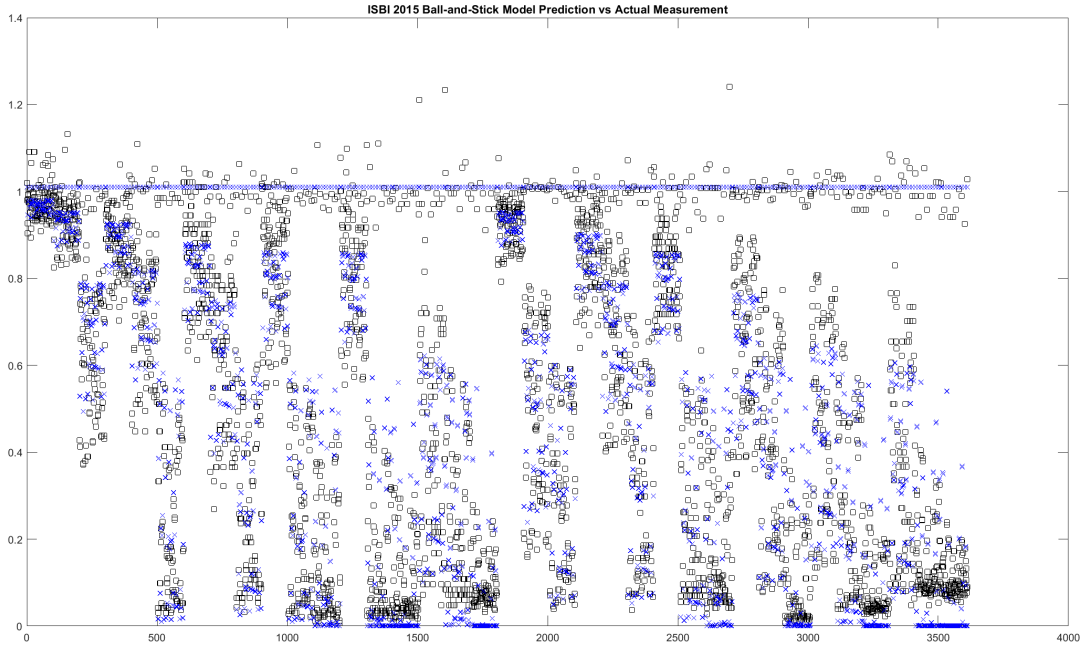

Figure 29: Ball-and-Stick model measurement (square) vs prediction (cross) for ISBI 2015 dataset.

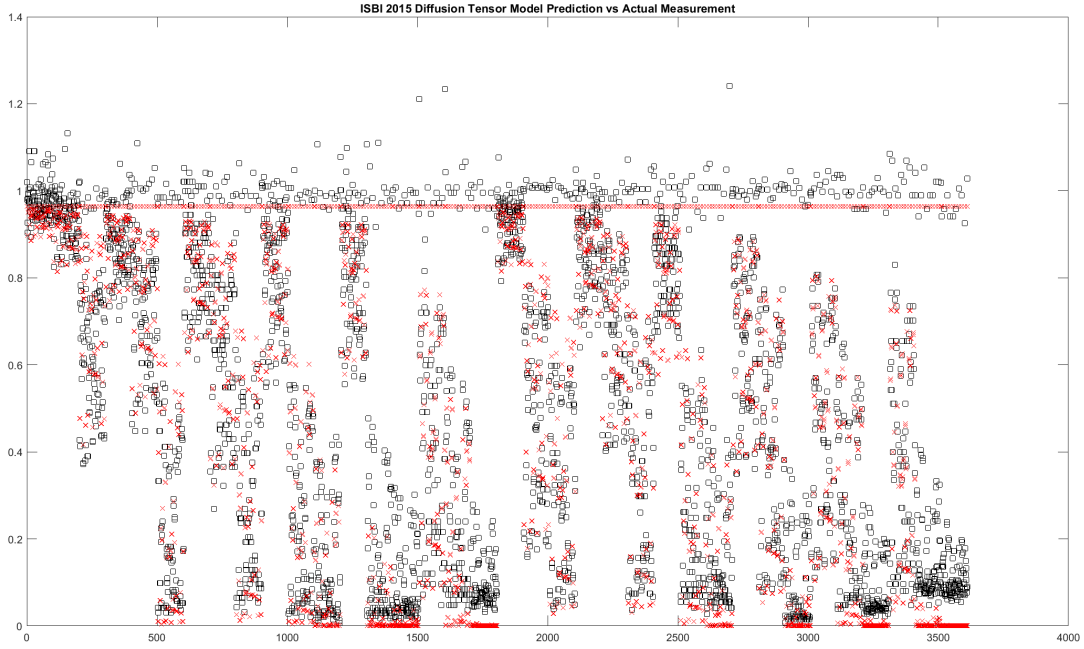

Figure 30: Diffusion tensor model measurement (square) vs prediction (cross) for ISBI 2015 dataset.

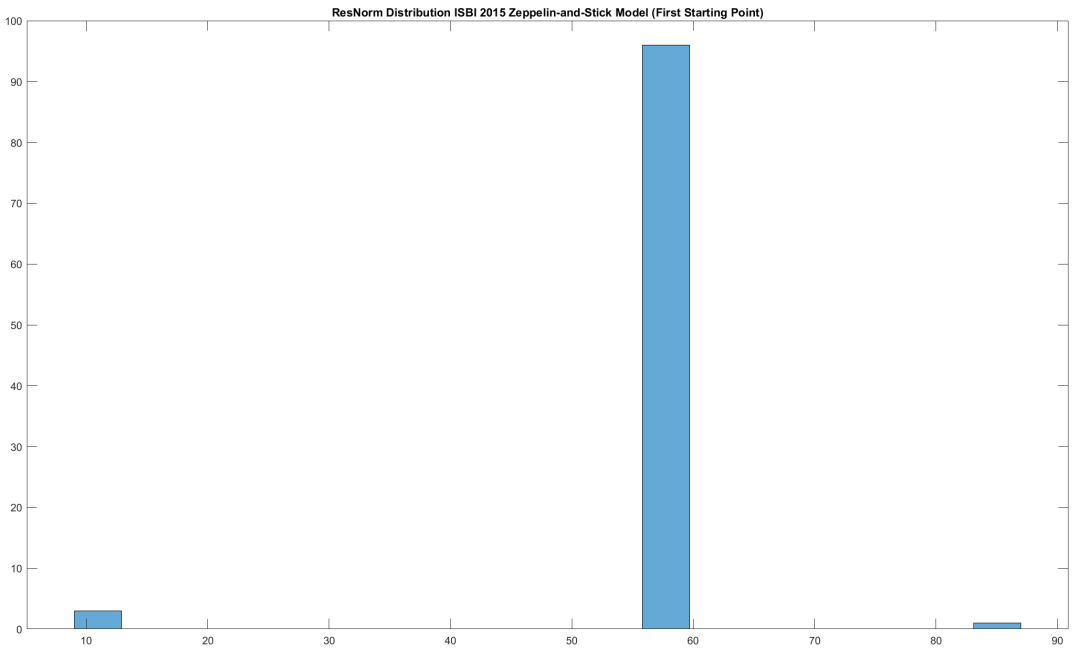

Figure 31: Zeppelin-and-Stick model first attempt resnorm distribution for ISBI 2015 dataset.

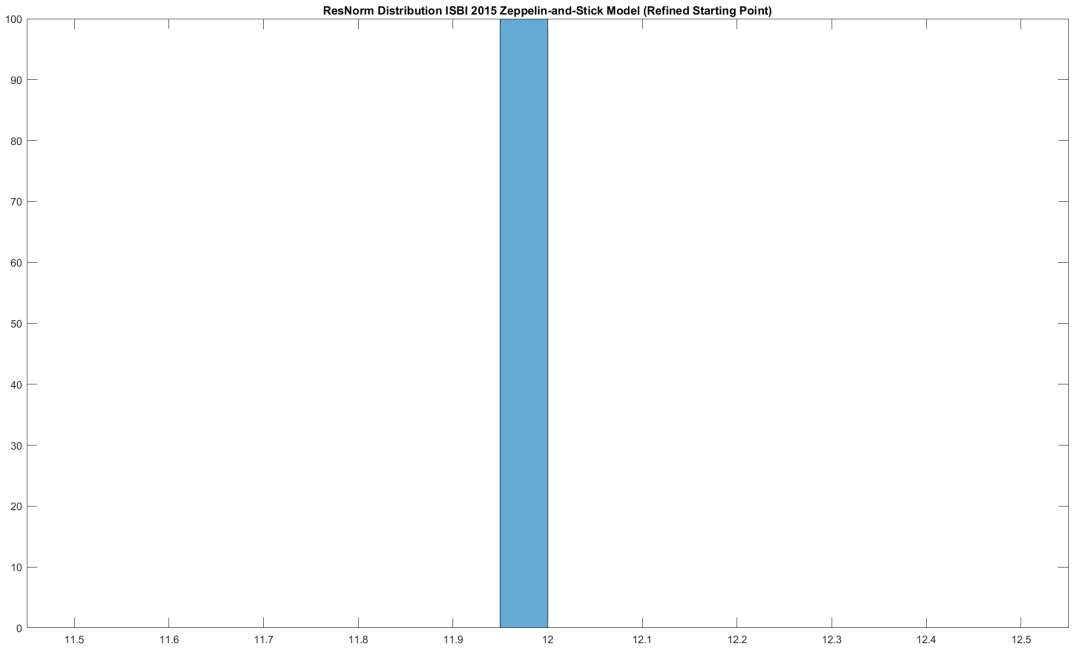

Figure 32: Zeppelin-and-Stick model refined resnorm distribution for ISBI 2015 dataset.

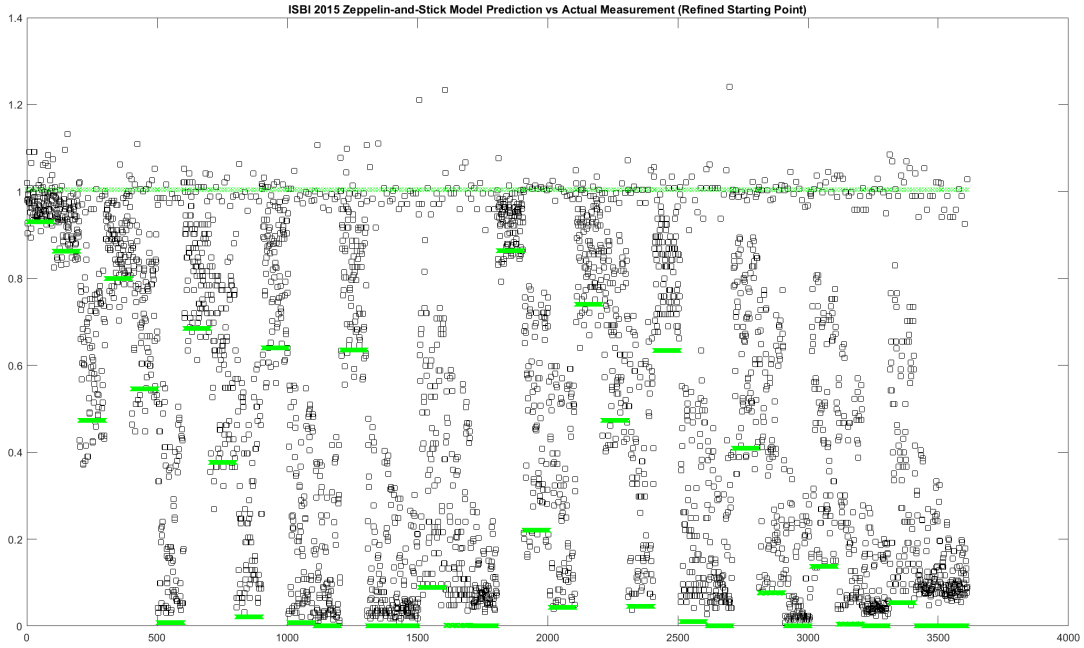

Figure 33: Zeppelin-and-Stick model refined measurement (square) vs prediction (cross) for ISBI 2015 dataset.

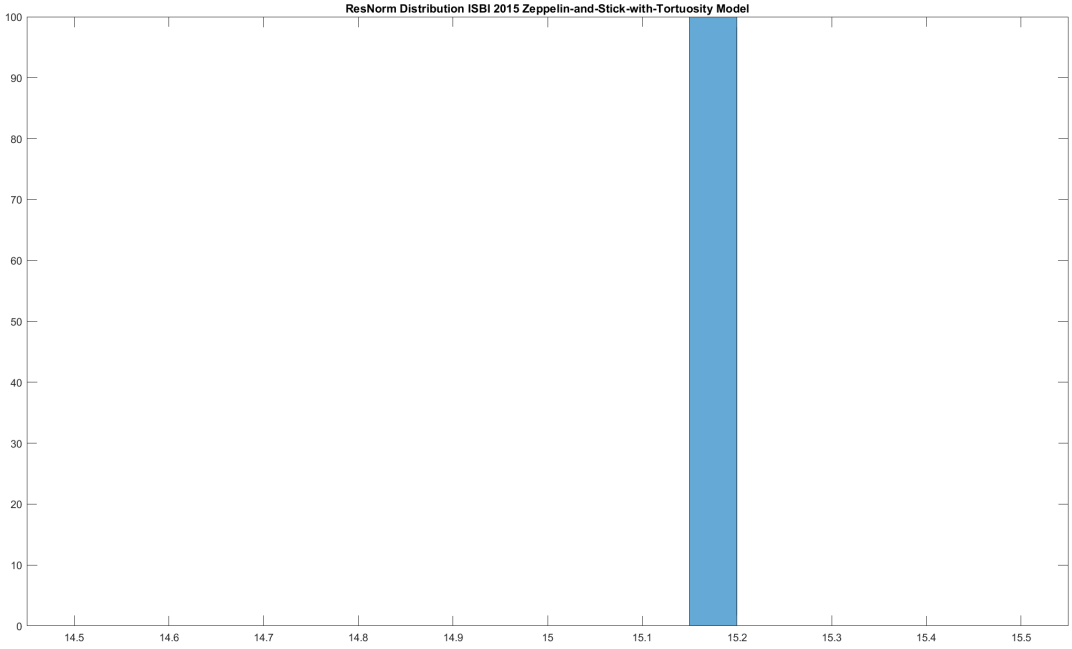

Figure 34: Zeppelin-and-Stick-with-Tortuosity model resnorm distribution for ISBI 2015 dataset.

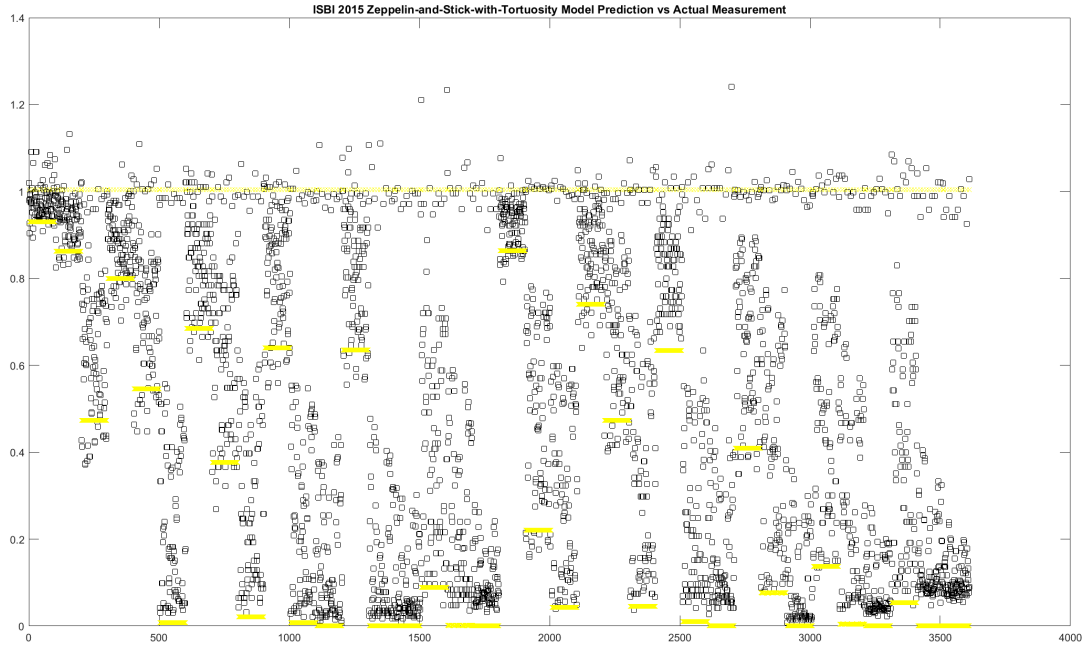

Figure 35: Zeppelin-and-Stick-with-Tortuosity model measurement (square) vs prediction (cross) for ISBI 2015 dataset.

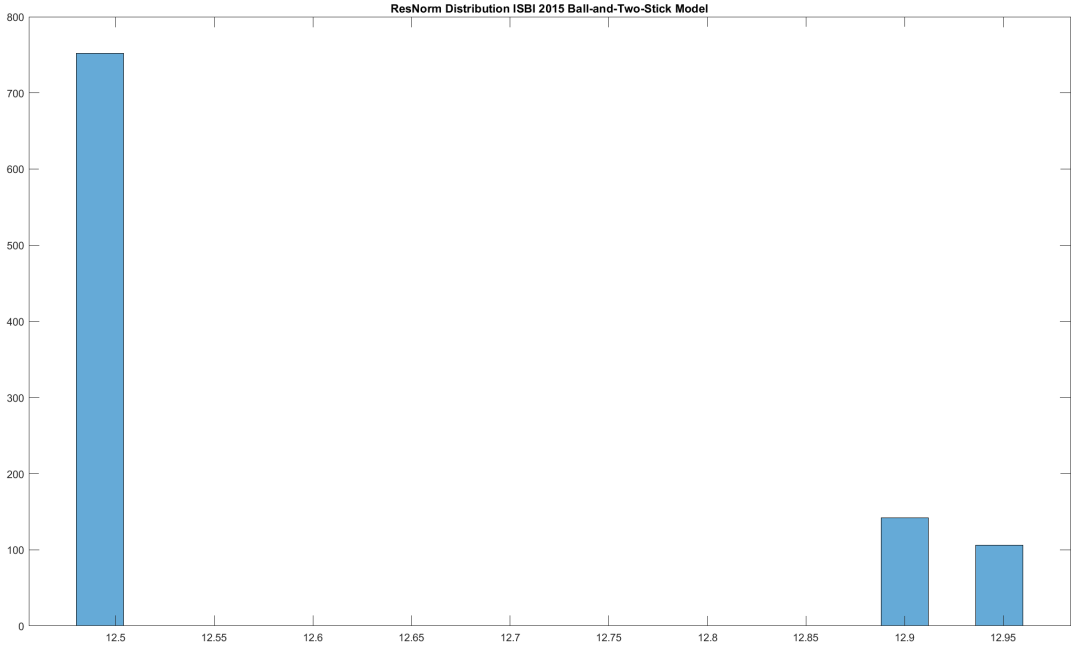

Figure 36: Ball-and-Two-Stick resnorm distribution for ISBI 2015 dataset.

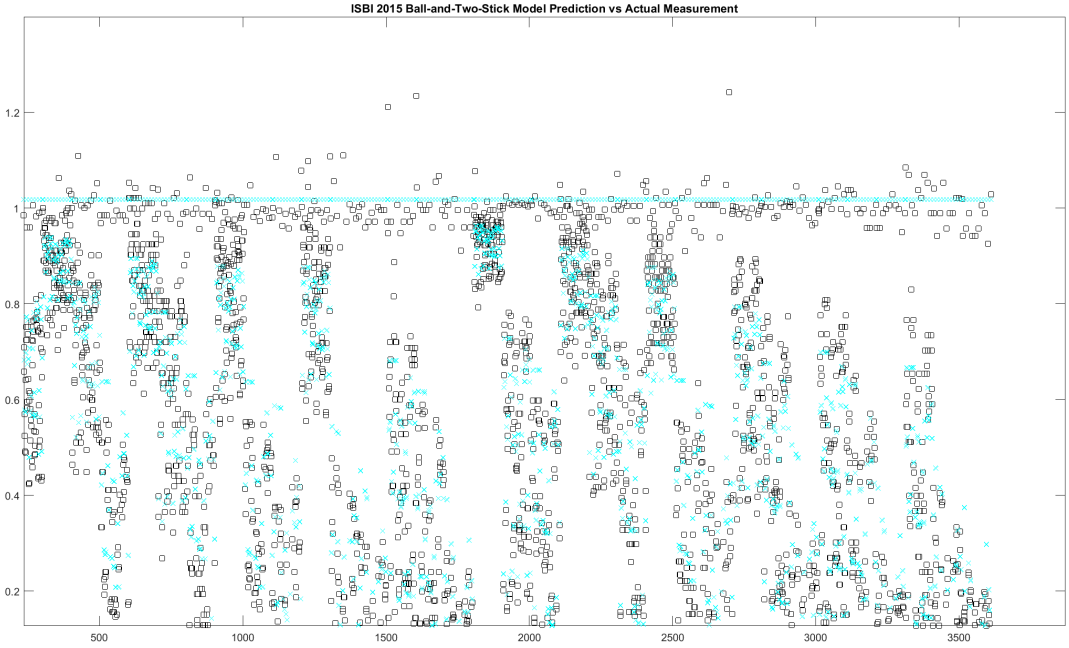

Figure 37: Ball-and-Two-Stick model measurement (square) vs prediction (cross) for ISBI 2015 dataset.

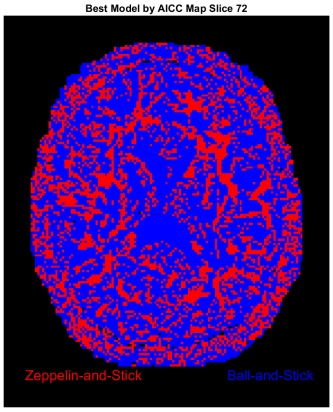

Figure 38: AICc mapping for the best model in HARDI slice 72

Table 9: Zeppelin-and-Stick best parameters for ISBI 2015 dataset.

Parameter	Value
ResNorm	1.1987e+01
S_0	1.0035e+00
$\lambda_1(d)$	1.5069e-03
λ_2	3.0288e-05
f	6.6643e-01
θ	-1.5447e+00
ϕ	-1.0097e-01

Table 10: Zeppelin-and-Stick-with-Tortuosity best parameters for ISBI 2015 dataset.

Parameter	Value
ResNorm	1.6562e+01
S_0	9.7358e-01
$\lambda_1(d)$	1.6369e-03
f	9.2344e-01
θ	-1.5479e+00
ϕ	-1.0298e-01

Table 11: Resnorm comparison across four models for ISBI 2015 dataset.

Model	ResNorm
Ball-and-Stick	1.5106e+01
Diffusion Tensor	1.8191e+01
Zeppelin-and-Stick	**1.1987e+01**
Zeppelin-and-Stick-with-Tortuosity	1.6562e+01

Table 12: Information criteria of four models for ISBI 2015 dataset.

Model	N parameters	AIC	BIC
Ball-and-Stick	6	-1.9771e+04	-3.9516e+04
Diffusion Tensor	8	-1.9095e+04	-3.8157e+04
Zeppelin-and-Stick	7	**-2.0604e+04**	**-4.1179e+04**
Zeppelin-and-Stick-with-Tortuosity	6	-1.9438e+04	-3.8852e+04

Table 13: Ball-and-Two-Stick best parameters for ISBI 2015 dataset.

Parameter	Value
ResNorm	1.1736e+01
S_0	1.0173e+00
d	1.7581e-03
f_1	3.2873e-01
θ_1	-1.8301e+00
ϕ_1	3.5563e-02
f_2	3.4824e-01
θ_2	-1.3022e+00
ϕ_2	-1.9979e-01

Table 14: Information criteria of five models for ISBI 2015 dataset.

Model	N parameters	AIC	BIC
Ball-and-Stick	6	-1.9771e+04	-3.9516e+04
Diffusion Tensor	8	-1.9095e+04	-3.8157e+04
Zeppelin-and-Stick	7	-2.0604e+04	-4.1179e+04
Zeppelin-and-Stick-with-Tortuosity	6	-1.9438e+04	-3.8852e+04
Ball-and-Two-Stick	9	**-2.0677e+04**	**-4.1315e+04**

Table 15: AIC and BIC comparison of best models for each voxel in ISBI 2015 dataset.

Voxel	**Best Model**	**AIC**	**BIC**
Voxel 1	Ball-and-Two-Stick	-2.0677e+04	-4.1315e+04
Voxel 2	Ball-and-Two-Stick	-2.0670e+04	-4.1302e+04
Voxel 3	Zeppelin-and-Stick	-1.9724e+04	-3.9419e+04
Voxel 4	Ball-and-Two-Stick	-1.9400e+04	-3.8761e+04
Voxel 5	Zeppelin-and-Stick	-2.0095e+04	-4.0160e+04
Voxel 6	Zeppelin-and-Stick	-2.0655e+04	-4.1281e+04

Table 16: Cross-validation results of best models for each fold in ISBI 2015 dataset.

Fold	**Ball-Stick**	**Diffusion Tensor**	**Zeppelin-Stick**	**Zeppelin-Stick-Tortuosity**	**Ball-Two-Stick**
Fold 1	2.1733e+00	1.1862e+01	1.7082e+00	2.3985e+00	1.7622e+00
Fold 2	2.4184e+00	7.5325e+00	1.9661e+00	2.9434e+00	2.1046e+00
Fold 3	2.4968e+00	8.5861e+00	1.9756e+00	2.6318e+00	1.9470e+00
Fold 4	2.6824e+00	1.1791e+01	2.1820e+00	2.7439e+00	2.0010e+00
Fold 5	2.7654e+00	6.6187e+00	2.1733e+00	2.8841e+00	2.0935e+00
Fold 6	2.6524e+00	8.5176e+00	2.0283e+00	2.9934e+00	1.9560e+00
Average	2.5314e+00	9.1513e+00	2.0056e+00	2.7658e+00	**1.9774e+00**
Minimum Folds	0	0	2	0	**4**

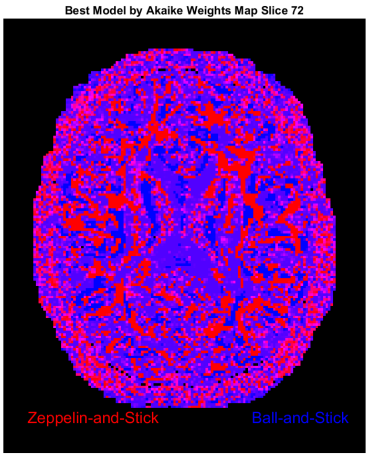

Figure 39: Akaike weighted AICc mapping for the best model in HARDI slice 72